Reactions of Anilines and Benzamides with a 14-Electron Iridium(I) Bis(phosphinite) Complex: N−H Oxidative Addition versus Lewis Base Coordination

Alison Cartwright Sykes, Peter White, and Maurice Brookhart*

Department of Chemistry, The University of North Carolina at Chapel Hill, Chapel Hill, North Carolina 27599-3290

Received December 15, 2005

Anilines react with (POCOP)Ir(C_6H_5)(H) (**12**; POCOP = 2,6-(OP*t*Bu$_2$)$_2$C$_6$H$_3$) to yield equilibrium mixtures of **12**, the Ir(I) σ-complexes (POCOP)Ir(NH_2Ar) (**13**), and the Ir(III) oxidative addition adducts (POCOP)Ir(H)(NHAr) (**14**). Quantitative studies of these equilibria for a series of anilines were carried out. Anilines possessing electron-withdrawing groups favor the Ir(III) oxidative addition adduct over the Ir(I) σ-complex. Low-temperature studies using *p*-chloroaniline show that the Ir(I) σ-complex is the kinetic product of the reaction and is likely the precursor to the Ir(III) oxidative addition adduct. Reductive elimination of complexes **14** in the presence of ethylene led to the corresponding anilines and the ethylene complex (POCOP)Ir(C_2H_4). Kinetic analysis of these reactions for **14e**−**g** bearing electron-withdrawing aryl groups (Ar- = *p*-$CF_3C_6H_4$-, C_6F_5-, 3,5-$(CF_3)_2C_6H_3$-) shows the rate is independent of ethylene concentration. The $\Delta G^{\ddagger}$ values for these reductive eliminations fall in the range of 21−22 kcal/mol. X-ray analysis establishes **14f** (Ar- = C_6F_5-) as a square-pyramidal complex with the hydride occupying the apical site. Reaction of **12** with benzamides **21a**,**b** yields quantitatively the Ir(III) oxidative addition adducts (POCOP)Ir(H)(NHC(O)Ar) (**22**). X-ray analysis of **22b** (Ar- = C_6F_5-) shows significant interaction of the carbonyl oxygen with Ir in the site trans to hydride. The barrier to reductive elimination of **22a**, 29 kcal/mol, is substantially higher than for complexes **14e**−**g**.

Introduction

Carbon−hydrogen bond activation by late transition metal complexes has received intense scrutiny over the past two decades since the classic work of Bergman,[1] Jones,[2] and Graham.[3] Fundamental studies, including kinetics, thermodynamics, and selectivities of the oxidative-addition reactions of C−H bonds to a variety of transition-metal centers together with theoretical investigations, have appeared.[4,5] More recently, these reactions have been incorporated into catalytic cycles, and there are now numerous useful catalytic organic transformations based on C−H bond activation reactions.[6−12]

Although N−H and C−H bonds exhibit similar homolytic bond strengths, much fewer investigations of late-metal activation of N−H bonds have been carried out.[13−16] Such studies could impact the rapidly growing number of metal-catalyzed transformations of amine and related compounds, including hydroaminations of alkenes, styrenes, dienes, and alkynes.[17−20] Some of these transformations appear to involve oxidative addition of N−H bonds,[21,22] while the mechanisms of many other transformations are unknown, but some could involve an N−H oxidative addition step.

An early instructive example of oxidative addition of N−H bonds to late transition metal centers was reported by Merola, who showed that the N−H bonds of pyrroles and indoles oxidatively add to the Ir(I) moiety (COD)$(PMe_3)_3Ir^+$, to yield the 18-electron, octahedral Ir(III) species illustrated in eq 1.[23]

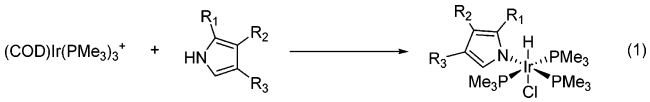

(1)

The Goldman, Jensen, and Kaska groups have shown that the 14-electron complex (PCP)Ir (**1**; PCP = 2,6-(CH_2-P*t*Bu$_2$)$_2$C$_6$H$_3$), generated from treatment of the dihydride (PCP)-Ir(H)$_2$ with acceptors such as *tert*-butylethylene, readily oxida-

* To whom correspondence should be addressed. E-mail: mbrookhart@unc.edu.

(1) Janowicz, A. H.; Bergman, R. G. *J. Am. Chem. Soc.* **1982**, *104*, 352.
(2) Jones, W. D.; Feher, F. *Organometallics* **1983**, *2*, 562.
(3) Hoyano, J. K.; McMaster, A. D.; Graham, W. A. G. *J. Am. Chem. Soc.* **1983**, *105*, 7190.
(4) Shilov, A. E.; Shul'pin, G. B. *Chem. Rev.* **1997**, *97*, 2879.
(5) Arndtsen, B. A.; Bergman, R. G.; Mobley, T. A.; Peterson, T. H. *Acc. Chem. Res.* **1995**, *28*, 154.
(6) Crabtree, R. H. *Dalton Trans.* **2001**, 2951.
(7) Crabtree, R. H. *Dalton Trans.* **2003**, 3985.
(8) Lersch, M.; Tilset, M. *Chem. Rev.* **2005**, *105*, 2471.
(9) Jun, C.-H.; Lee, J. H. *Pure Appl. Chem.* **2004**, *76*, 577.
(10) Ishiyama, T. *Kagaku to Kogyo (Tokyo)* **2003**, *56*, 1237.
(11) Kakiuchi, F.; Chatani, N. *Adv. Synth. Catal.* **2003**, *345*, 1077.
(12) Labinger, J. A.; Bercaw, J. E. *Nature (London)* **2002**, *417*, 507.
(13) Hartwig, J. F.; Andersen, R. A.; Bergman, R. G. *Organometallics* **1991**, *10*, 1875.
(14) Glueck, D. S.; Winslow, L. J. N.; Bergman, R. G. *Organometallics* **1991**, *10*, 1462.
(15) Bryndza, H. E.; Tam, W. *Chem. Rev.* **1988**, *88*, 1163.
(16) Fulton, J. R.; Holland, A. W.; Fox, D. J.; Bergman, R. G. *Acc. Chem. Res.* **2002**, *35*, 44.
(17) Utsunomiya, M.; Hartwig, J. F. *J. Am. Chem. Soc.* **2004**, *126*, 2702.
(18) Hartwig, J. F. *Pure Appl. Chem.* **2004**, *76*, 507.
(19) Beller, M.; Breindl, C.; Eichberger, M.; Hartung, C. G.; Seayad, J.; Thiel, O. R.; Tillack, A.; Trauthwein, H. *Synlett* **2002**, 1579.
(20) Utsunomiya, M.; Kuwano, R.; Kawatsura, M.; Hartwig, J. F. *J. Am. Chem. Soc.* **2003**, *125*, 5608.
(21) Uchimaru, Y. *Chem. Commun.* **1999**, 1133.
(22) Casalnuovo, A. L.; Calabrese, J. C.; Milstein, D. *J. Am. Chem. Soc.* **1988**, *110*, 6738.
(23) Ladipo, F. T.; Merola, J. S. *Inorg. Chem.* **1990**, *29*, 4172.

10.1021/om051070n CCC: $33.50
Publication on Web 03/03/2006

tively adds C−H bonds of alkanes and arenes.[24,25] Such species are highly active for catalytic transfer dehydrogenation of alkanes and can also be used for synthesis of enamines through transfer dehydrogenation of tertiary amines.[26] Goldman and Hartwig have recently observed that the (PCP)Ir complex **1** oxidatively adds the N−H bond of aniline to produce the Ir(III) anilino hydride **2**, as shown in eq 2.[27] In benzene, adduct

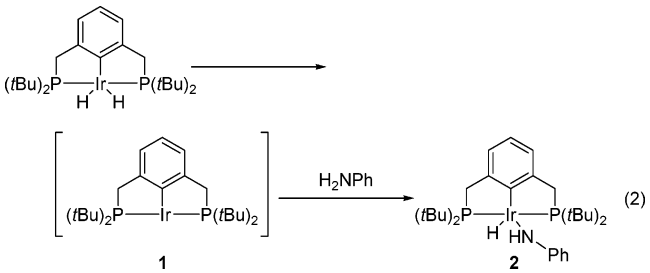

(2)

2 equilibrates with the phenyl hydride complex **3**. The equilibrium favors the anilino hydride complex with $K_{eq} = 105$ at 22 °C (eq 3).

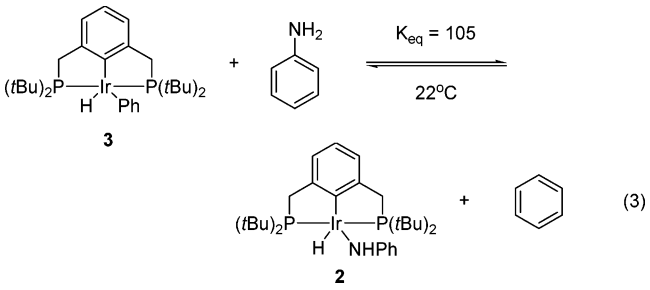

(3)

Attempted oxidative addition of the better σ-donor ammonia results in the Ir(I) ammonia complex **4**. The amido hydride **5** can be independently generated by dehydrochlorination of **6** at −78 °C. Warming to 25 °C resulted in conversion to ammonia complex **4**, indicating that thermodynamically the ammonia complex is favored over the amido hydride (eq 4). When a more

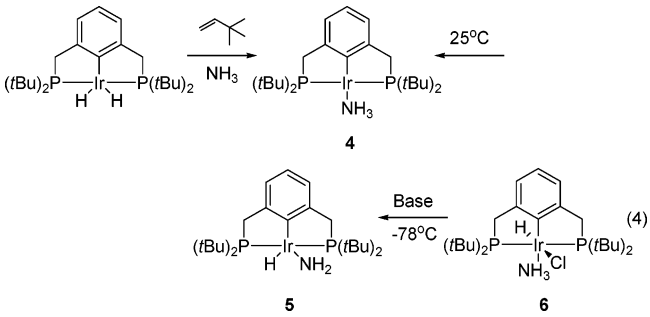

(4)

electron-donating saturated backbone is incorporated in the pincer ligand, oxidative addition of ammonia occurs rather than simple coordination.[28] Treatment of **7** with ammonia gives the Ir(III) amido hydride in high yields at 25 °C (eq 5).

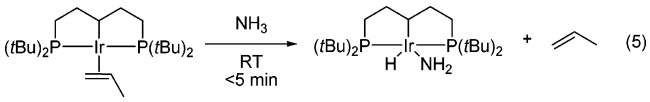

(5)

Our laboratory[29−31] has investigated the chemistry of more electron-deficient Ir pincer complexes based on the bis(phosphinite) ligand POCOP (=2,6-(OP*t*Bu$_2$)$_2$C$_6$H$_3$). The highly active 14-electron complex **10** can be conveniently generated in situ by treatment of the hydrido chloride **9** with sodium *tert*-butoxide (eq 6). Generation of **10** in a cyclooctane/*tert*-

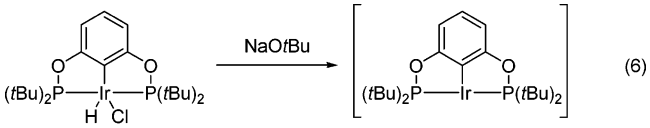

(6)

butylethylene mixture produces a highly active catalyst system for transfer dehydrogenation and production of cyclooctene and cyclooctadiene (eq 7). Detailed mechanistic studies of this

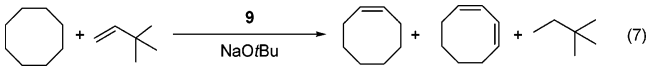

(7)

system have complemented the studies of Goldman on **1** and provided interesting contrasts, suggesting that the phosphinite POCOP system prefers the Ir(I) oxidation state relative to the PCP systems.[29−31]

In this paper we report the reaction of a series of substituted anilines and benzamides with the phosphinite pincer complex **10**. In the case of the anilines, the Ir(III) oxidative addition adduct, the Ir(I) σ-complex, or a mix of these products is formed, depending on the nature of the para substituent. Rates of reductive elimination of the Ir(III) species have been measured, as well as the equilibria in benzene between the aniline adducts and the phenyl hydride. Information on the mechanism of reductive elimination was attained through the study of low-temperature reactions of both the *p*-chloroaniline and the *p*-methoxyaniline complexes.

Results and Discussion

(I) Reaction of (POCOP)Ir Pincer complexes with Various Anilines (11a−g). (a) Equilibration of (POCOP)Ir(H)(C$_6$H$_5$) (12) with (POCOP)Ir(NH$_2$Ar) (13) and (POCOP)Ir(H)-NHAr) (14). Reactions of anilines shown in Chart 1 with the

Chart 1. Anilines of Varying Electron-Withdrawing and -Donating Ability (11a−g)

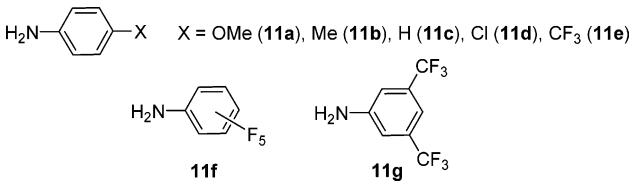

14-electron (POCOP)Ir pincer complex **10** were carried out

(24) Liu, F.; Pak, E. B.; Singh, B.; Jensen, C. M.; Goldman, A. S. *J. Am. Chem. Soc.* **1999**, *121*, 4086.

(25) Kanzelberger, M.; Singh, B.; Czerw, M.; Krogh-Jespersen, K.; Goldman, A. S. *J. Am. Chem. Soc.* **2000**, *122*, 11017.

(26) Zhang, X.; Fried, A.; Knapp, S.; Goldman, A. S. *Chem. Commun.* **2003**, 2060.

(27) Kanzelberger, M.; Zhang, X.; Emge, T. J.; Goldman, A. S.; Zhao, J.; Incarvito, C.; Hartwig, J. F. *J. Am. Chem. Soc.* **2003**, *125*, 13644.

(28) Zhao, J.; Goldman, A. S.; Hartwig, J. F. *Science (Washington, DC)* **2005**, *307*, 1080.

(29) Goettker-Schnetmann, I.; Brookhart, M. *J. Am. Chem. Soc.* **2004**, *126*, 9330.

Scheme 1. Equillibria between (POCOP)Ir(H)(Ph) (12), (POCOP)Ir(NH_2Ar) (13), and (POCOP)Ir(H)(NHAr) (14)

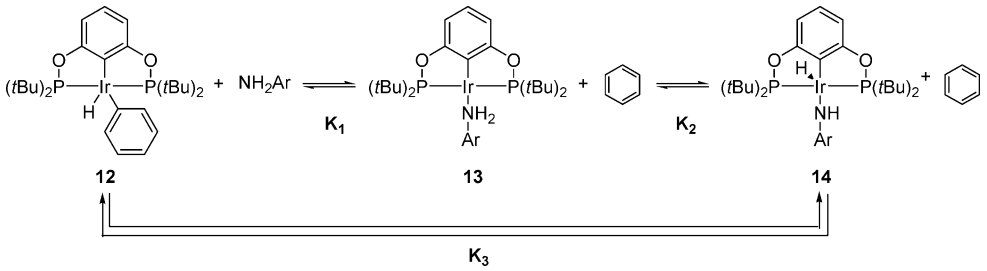

Table 1. Equilibrium Constants[a] for 12 + NH_2Ar ⇌ 13 + Benzene ⇌ 14 + Benzene at 25 °C

aniline (**11**)	K_1	K_2	K_3 (=K_1K_2)
a	1130	*b*	*b*
b	456	0.04	18
c	188	0.1	19
d	55	1	55
e	*c*	*c*	260
f	*c*	*c*	2190
g	*c*	*c*	2770

[a] Equilibrium values are based on an average of two to three runs. [b] Concentration of **14a** too low to detect. [c] Concentrations of **13e-g** too low to detect.

by treatment of the hydrochloride complex **9** with NaO*t*Bu and anilines **11a−g** in benzene at room temperature for 1.5 h. The phenyl hydride complex **12** is in rapid equilibrium with **10**[31] and thus reacts with the aniline to form either the *σ*-complex **13** or the oxidative addition adduct **14**. The three species **12−14**, depicted in Scheme 1, are all in equilibrium at 25 °C. ^{31}P NMR spectroscopy was used to determine the ratios of the three species. Complex **12** exhibits a ^{31}P shift at 182 ppm,[31] while the Ir(I) *σ*-complexes show resonances in the 173.4−173.6 ppm range and ^{31}P signals of the Ir(III) oxidative addition adducts occur in the 171.7−173.3 ppm range. The ^{1}H NMR data, as well as a crystal structure of **14f** (see below), confirm the structural assignments of these species. The *σ*-complexes exhibit a broad 2H resonance around 5.2 ppm, distinct from the ArNH_2 resonance for free anilines, indicating that these species are exchanging slowly on the NMR time scale. The ArNHIr ^{1}H signals for the oxidative addition adducts appear in the 3.0−5.6 ppm range and are paired with a Ir−H triplet (J_{PH} = 12.6−13.5 Hz) at high fields (−34.1 to −42.2 ppm range). The Ir hydride signal for **12** cannot be detected at room temperature, due to rapid exchange with benzene via complex **10**.[31]

The equilibrium constants K_1, K_2, and K_3, measured by ^{31}P NMR spectroscopy at 25 °C, are summarized in Table 1. For the electron-rich *p*-methoxyaniline **11a**, only the Ir(I) *σ* adduct **13a** can be observed. As the substituents become more electron-withdrawing, the Ir(III) oxidative addition adduct becomes increasingly favored. For example, a 1:1 ratio of Ir(III):Ir(I) is now observed for *p*-chloroaniline **11d**. For even less electron-rich anilines **11e−g**, the Ir(I) species can no longer be spectroscopically detected and K_2 cannot be measured. The equilibrium constants K_3 between the aryl hydride and Ir(III) complexes can still be determined, since benzene is in large excess relative to aniline and **12** can be detected. The reasons for the trends in these substituent effects will be discussed below.

To confirm the structures of the anilino hydrides, a single-crystal X-ray diffraction analysis of a crystal of **14f** grown from pentane at −35 °C was carried out. An ORTEP diagram of the structure, including key bond distances and angles, is shown in Figure 1. The complex is square pyramidal, with the hydride in an apical position. There is an empty coordination site trans to the hydride. The dihedral angle Ir(1)−N(1)−C(2)−C(7) is 32.5°, indicating the arene ring sits approximately perpendicular to the square plane and the filled p orbital on nitrogen lies parallel to the square plane. The N−H bond lies anti to the Ir−H bond (H−Ir(1)−N(1)−H dihedral angle 177.3°), and thus, there can be no N−H- - -H−Ir interaction as seen in related systems.[32]

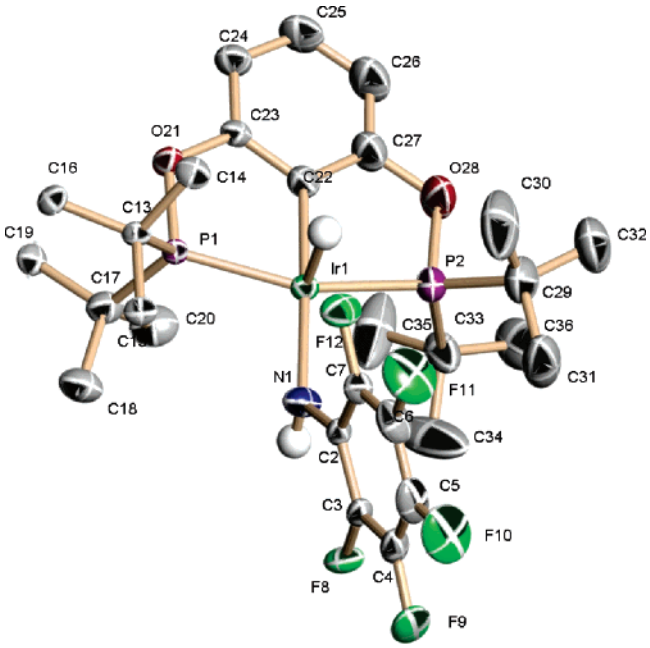

Figure 1. ORTEP diagram of **14f**. Only the hydrogens on iridium and nitrogen are shown for clarity. Key bond distances (Å) and bond angles (deg): Ir(1)−N(1) = 2.145, N(1)−C(2) = 1.348, Ir(1)−C(22) = 2.013, Ir(1)−P(1) = 2.294, Ir(1)−P(2) = 2.309; C(22)−Ir(1)−N(1) = 177.32, P(1)−Ir(1)−N(1) 99.20, P(2)−Ir(1)−N(1) 101.42, Ir(1)−N(1)−C(2)−C(7) = 32.5, H−Ir(1)−N(1)−H 177.31.

It is worth noting that the crystal structure of **14f** is representative of the (POCOP)Ir^{III} complexes of the electron-withdrawing anilines **14e−g**. The ^{1}H resonance of the hydride in these complexes falls between −41 and −43 ppm, which seems to be characteristic of hydride shifts in these (POCOP)Ir pincer complexes when there is an empty coordination site trans to the hydride. However, for the (POCOP)Ir^{III} complexes of the less electron-withdrawing anilines **14b−d** the chemical shift for the hydride falls between −33.3 and −35.9 ppm. This surprisingly downfield chemical shift might be indicative of a change in orientation of the aniline substituent, where the

(30) Goettker-Schnetmann, I.; White, P.; Brookhart, M. *J. Am. Chem. Soc.* **2004**, *126*, 1804.
(31) Goettker-Schnetmann, I.; White, P. S.; Brookhart, M. *Organometallics* **2004**, *23*, 1766.
(32) Crabtree, R. H. *Science (Washington, D.C.)* **1998**, *282*, 2000.

Scheme 2. Comparison of the Reactions of (PCP)Ir(H)(Ph) (3) and (POCOP)Ir(H)(Ph) (10) with $NH_2C_6H_5$

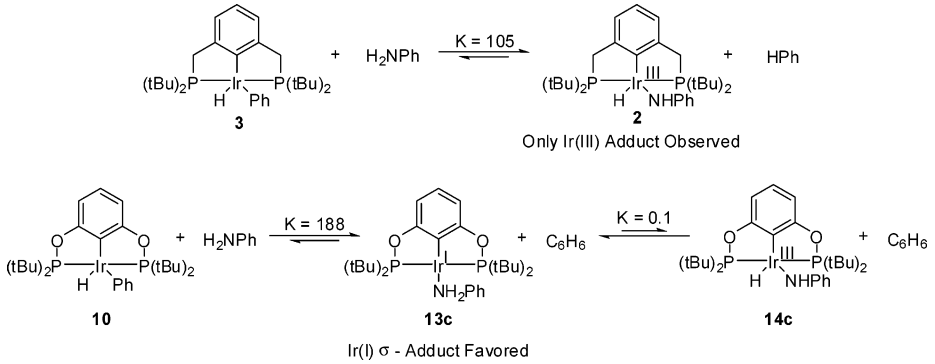

hydride and the *N*-hydrogen are cis to each other with a possible hydrogen-bonding interaction.[32] A corresponding shift in the ArN*H* signal occurs on moving from ca. 3.0−4.4 ppm in the adducts involving electron-withdrawing anilines (**14e**−**g**) to 5.6 ppm for the *p*-chloroaniline adduct **14d**.

When the equilibrium data for reaction with aniline are compared with those of Goldman and Hartwig,[27] it is clear that the more electron-withdrawing (POCOP) phosphinite Ir system more strongly prefers the Ir(I) oxidation state relative to the (PCP)Ir system. At room temperature, the reaction of **1** with $H_2NC_6H_5$ favors the oxidative addition product and forms only the Ir(III) anilino hydride complex. In benzene solution, an equilibrium is established between (PCP)Ir(H)(NHC_6H_5) and (PCP)Ir(H)(C_6H_5) with a K_{eq} value of 105 favoring the formation of the iridium anilino complex.[27] In the POCOP system, reaction of **10** with $NH_2C_6H_5$ favors the Ir(I) σ-complex with an Ir(I):Ir(III) complex equilibrium ratio of ca. 10:1 (see Scheme 2). These results are also supported by IR data. Comparison of the IR stretching frequencies of coordinated carbon monoxide in (POCOP)Ir(CO) (**15**; ν_{CO} 1949 cm^{-1})[31] and (PCP)Ir(CO) (**16**; ν_{CO} 1927.7 cm^{-1})[33] shows a higher frequency C≡O stretch for **15** than for **16**, indicating that the more electron-withdrawing ligand leads to a more electron-deficient metal center.

The increasing donor ability of the lone pair of electrons on the aniline is reflected, as expected, by the increasing stability of the Ir(I) σ-aniline complexes relative to the Ir(III) phenyl hydride complex (compare K_1 values, Table 1). The stability of the Ir(III) anilino hydride complexes relative to the Ir(III) phenyl hydride increases as the arene ring of the aniline becomes more electron withdrawing (K_3 values). This behavior can be rationalized in two ways. In the d^6 Ir(III) complexes **14**, all the d_π orbitals are filled and thus there are unfavorable p_π−d_π interactions[34,35] in **14e**−**g**. The crystal structure of **14f** shows that the Ir−N−C plane lies perpendicular to the Ir(III) square plane. As illustrated in Figure 2, there is repulsive interaction between the filled Ir d_{xy} orbital and the filled N p_y orbital. As the arene becomes more electron-withdrawing, the energy of the p_y orbital is lowered and the destabilizing interaction is reduced. This could account for the substituent effect on relative stabilities. An alternative view is that the electron-withdrawing substituents stabilize the negative charge on the anilino ligand, enhancing the electrostatic interaction between the metal and the anilino group, thus strengthening the Ir−N bond.[36,37]

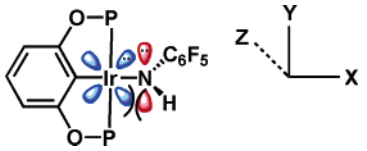

Figure 2. The destabilizing interaction between the filled N π orbital (p_y) and the filled Ir d_{xy} orbital (apical hydride not shown).

(b) Rates of Oxidative Addition of Anilines to (POCOP) Iridium Pincer Complexes. Low-temperature ^1H and ^{31}P studies showed that in the case of *p*-chloroaniline (which yields a 1:1 equilibrium mixture of **13d** and **14d**) the kinetic product of reaction with **10** is the σ-complex **13d**. Generation of the tolyl hydride complexes **17** (a mixture of the meta and *para* isomers[31]) in toluene was achieved in the usual way by reaction of the hydrochloride complex in toluene with NaO*t*Bu. Treatment of this solution with excess *p*-chloroaniline (10 equiv) at −50 °C initially yields only the σ complex **13d** (eq 8). Slow

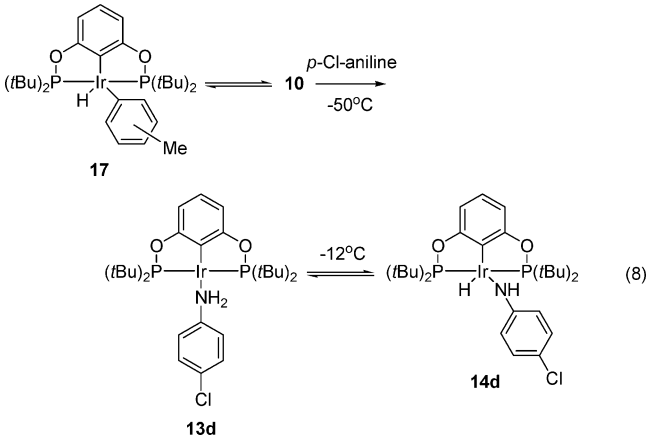

(8)

formation of the oxidative addition product **14d** is observed at this temperature. While it seems likely that the oxidative addition occurs directly from the σ complex, we have no direct proof of this. After formation of the σ complex **13d**, the rate of oxidative addition of the *p*-chloroaniline to form **14d** was measured at −12 °C via ^1H low-temperature NMR spectroscopy. The first-order rate constant was found to be 4.8×10^{-4} s^{-1} with $\Delta G^{\ddagger} = 19.7$ kcal/mol.

Similar low-temperature experiments were conducted with 3,5-bis(trifluoromethyl)aniline (**11g**). At the highest achievable concentrations of aniline, a trace of a species tentatively assigned to the σ complex (δ(^{31}P) 173.2, maximum concentration ca.

(33) Krogh-Jespersen, K.; Czerw, M.; Zhu, K.; Singh, B.; Kanzelberger, M.; Darji, N.; Achord, P. D.; Renkema, K. B.; Goldman, A. S. *J. Am. Chem. Soc.* **2002**, *124*, 10797.
(34) Crabtree, R. H. *The Organometallic Chemistry of the Transition Metals*, 3rd ed.; Wiley: New York, 2001.
(35) Caulton, K. G. *New J. Chem.* **1994**, *18*, 25.
(36) Holland, P. L.; Andersen, R. A.; Bergman, R. G. *Comments Inorg. Chem.* **1999**, *21*, 115.
(37) Holland, P. L.; Andersen, R. A.; Bergman, R. G.; Huang, J.; Nolan, S. P. *J. Am. Chem. Soc.* **1997**, *119*, 12800.

Scheme 3. Possible Mechanism for Oxidative Addition of 11g

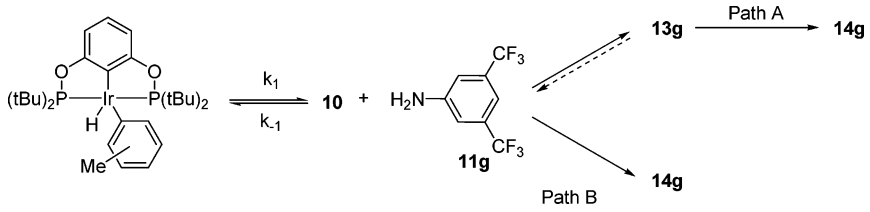

3.0%) could be detected as a transient during reactions carried out at −37 °C (Scheme 3). These results are consistent with formation of the *σ*-complex as the kinetic product, which never builds up to significant concentrations due to rapid oxidative addition to form **14g** (path A). Again, we cannot rule out direct formation of **14g** from reaction of **10** with **11g** (path B).

(c) Rates of Reductive Elimination of Electron-withdrawing Anilines from Five-Coordinate (POCOP) Iridium Pincer Complexes using Ethylene as a Trapping Ligand. The rates of reductive elimination of **14e**−**g** were measured by heating the Ir(III) adducts in the presence of ethylene as a trapping ligand, L, to form the iridium(I) ethylene adduct **18**, as shown below in eq 9. Complexes **14e**−**g** were chosen for study, since

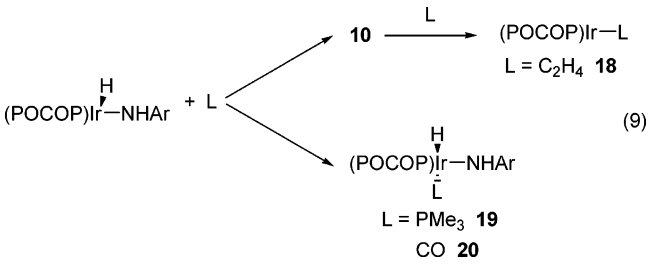

(9)

K_2 and K_3 are sufficiently large that the Ir(III) complexes can be prepared cleanly with no contamination by aryl hydride **12** or Ir(I) complexes. The trapping ligand must be chosen so that the 18-electron Ir(III) six-coordinate complex is not formed. A survey of several trapping ligands revealed that ethylene was ideal for this purpose (PMe_3 and carbon monoxide form the octahedral complexes **19**[38] and **20** prior to reductive elimination; see below).

The disappearance rates of adducts **14e**−**g** were measured at 9 °C in the presence of excess ethylene and found to be independent of ethylene concentration (eq 10). Measured rate

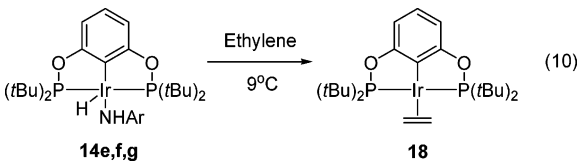

(10)

constants and free energies of activation are summarized in Table 2.

The reductive eliminations follow the same trend as the equilibrium reactions above; the more electron-withdrawing aniline reductively eliminates more slowly (Table 2). This is also evident by comparing the free energies of activation, $\Delta G^{\ddagger}$ values, for the reductive eliminations. As the electron-withdrawing ability of the aniline increases, the $\Delta G^{\ddagger}$ value also increases from 20.8 kcal/mol for aniline **11e** to 22.1 kcal for **11g**.

(38) Formed by reaction of in situ generated **14f** followed by addition of PMe_3 at −40 °C. Key NMR resonances include the following: ^{1}H NMR (400 MHz, C_7D_8) δ −11.9 (dt, Ir-*H*, J_{P-H} = 149.1 Hz (trans), J_{P-H} = 23.4 Hz (cis); ^{31}P NMR (162 MHz, C_7D_8) δ 169.6 (m, 2P), −57.1 (m, 1P).

Table 2. Rates of Reductive Elimination of Anilines (11e−g) from (POCOP)Ir(H)(NHAr) at 9 °C in Toluene

Ir(III) complex	C_2H_4 concn, M	k, 10^4 s^{-1}	av k, 10^4 s^{-1}	$\Delta G^{\ddagger}$, kcal/mol
14e (0.022 M)	0.087	4.0	4.2	20.8
	0.28	4.4		
14f (0.022 M)	0.022	3.0	2.8	21.1
	0.19	2.6		
	1.1	2.8		
14g (0.036 M)	0.18	0.42	0.45	22.1
	0.34	0.47		

To determine if these barriers are the true barriers for reductive elimination of anilines from **14e**−**g**, several mechanistic scenarios, consistent with the observation that the rates of formation of ethylene complex **18** are independent of ethylene concentration, were considered. These are summarized in cases A−C in Scheme 4. In case A, slow reductive elimination leads *directly* to **10**, followed by fast trapping by ethylene leading to formation of the ethylene complex **18**. In view of the above experiments with *p*-chloroaniline, which suggest that the *σ*-complex is the precursor to oxidative addition adducts, case A seems less likely than cases in which reductive elimination initially leads to the *σ*-complex. In case B, the *σ*-complex **13** is the precursor to **10**, which is then rapidly trapped by ethylene. It is possible that the rate of formation of **13** is rate-determining (i.e. $k_2 > k_1, k_{-1}$) or that **13** and **14** are in equilibrium followed by slow formation of **10** ($k_2 < k_{-1}$). (In this latter case, the measured $\Delta G^{\ddagger}$ values do not correspond to the true barriers for reductive elimination of **14e**−**g**.) In case C, formation of **13** is rate-determining, followed by rapid associative displacement of the aniline by ethylene.

To probe whether displacement of anilines from **13** by ethylene is associative or dissociative, we examined the reaction of **13a**, a system for which the *σ*-complex **13a** can be generated free of the Ir(III) oxidative addition adduct **14a**. Generation of **13a** in toluene at room temperature followed by exposure to ethylene at −8 °C results in quantitative formation of ethylene complex **18** (eq 11).

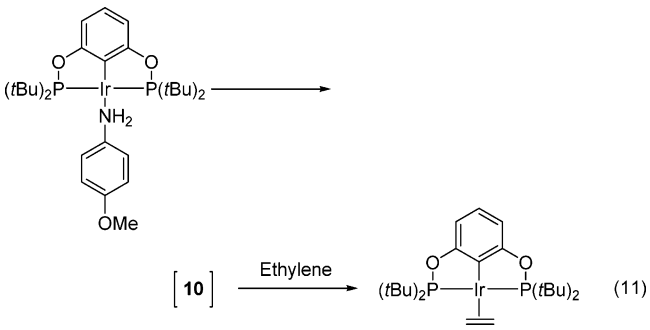

(11)

Using 0.015−0.019 M **13a** and excess ethylene concentrations of 0.25 and 0.48 M, clean first-order kinetics are observed at −8 °C with measured rate constants of 3.3×10^{-4} and 2.7×10^{-4} s^{-1}, respectively. No dependence of the rate on ethylene

Scheme 4

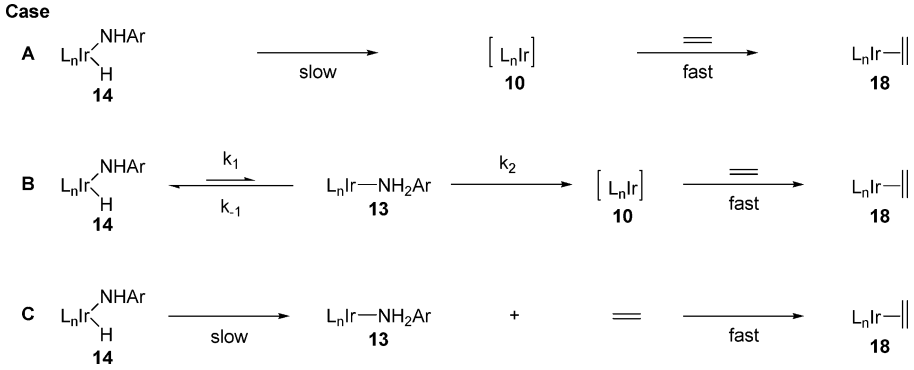

is observed, which implies that dissociation of *p*-methoxyaniline from **13a** is rate-determining with a free energy of activation, $\Delta G^{\ddagger}$, of 19.8 kcal/mol. This result rules out case C above and indicates case B as the most likely choice.

In examining case B more closely, it is instructive to consider free energy diagrams for both the *p*-chloroaniline system **13d**/**14d** and **14e**−**g** (for simplicity consider **14f** as representative of **14e**−**g**) (Figure 3). In the case of **13d**/**14d**, $K_{eq} = 1$; therefore, barriers for reductive elimination and oxidative addition are the same, 19.7 kcal/mol. Now consider **14f**. Since **14f** is somewhat more stable than **13f**, one would expect the $\Delta G^{\ddagger}_1$ value to be slightly greater than 19.7 kcal/mol, e.g. 19.7 + δ, and $\Delta G^{\ddagger}_{-1}$ to be slightly less, 19.7 − δ', as shown in Figure 3. Since $(CF_3)_2C_6H_3NH_2$ is a poorer donor than *p*-methoxyaniline, the barrier for dissociation from (POCOP)Ir should be somewhat less than the 19.8 kcal/mol measured for **13a**, designated in Figure 3 as 19.8 − δ''. It is difficult to predict whether δ' or δ'' is larger and thus which transition state, TS_1 or TS_2, is higher in energy, but it is likely that the difference is quite small. The $\Delta G^{\ddagger}_1$ value for **14f** cannot exceed 21.1 kcal/mol (see Table 1) but is certainly greater than 19.7 kcal/mol and thus is narrowly bracketed. In view of this analysis the $\Delta G^{\ddagger}$ values in Table 1 likely reflect fairly accurately the barriers for reductive elimination of **14e**−**g**.

It is informative to compare the barriers of reductive elimination observed here, which are in the 21−22 kcal/mol range, to the barrier of reductive elimination of (POCOP)Ir(H)(Ar′) (Ar′- = 3,5-$Me_2C_6H_3$-) of 14.1 kcal/mol.[39] This likely reflects a stronger Ir−N bond relative to the Ir−C bond.[36]

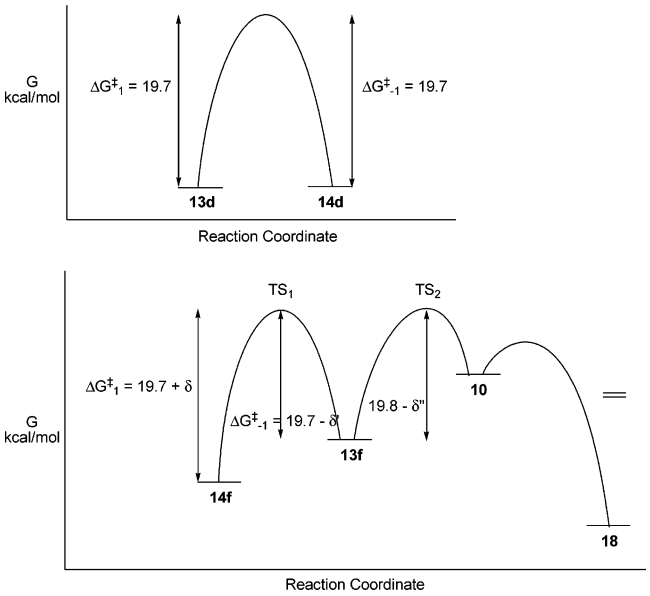

Figure 3. Reaction coordinate diagram for interconversion of **13d** and **14d** and conversion of **14f** to **18**.

(d) Reaction of (POCOP)Ir(H)(NHAr) Complexes (14e,f) with Carbon Monoxide. Generation of the tolyl hydrides **17** at −78 °C as described above followed by treatment with $C_6F_5NH_2$ (ca. 1.1 equiv) and CO resulted in formation of (POCOP)Ir(CO)(H)(NHC_6F_5) (**20f**) as the major product via CO trapping of **14f**. (Minor amounts of (POCOP)IrCO (**15**) are formed, presumably by CO displacement of aniline from (POCOP)Ir($NH_2C_6F_5$), since reductive elimination of aniline from either **14f** or **20f** is very slow at −78 °C.) Removal of toluene and addition of a minimal amount of pentane at −78 °C resulted in the precipitation of **20f** in low yield. Key NMR parameters of **20f** include a ^{31}P signal at 157 ppm and a ^{1}H resonance for the iridium hydride at −8.6 ppm. The downfield hydride shift is indicative of ligand coordination trans to the apical hydride. A solution of **20f** in toluene at 25 °C undergoes slow reductive elimination; (POCOP)Ir(CO) and free pentafluoroaniline are visible by ^{1}H NMR spectroscopy after 18 h.

X-ray-quality crystals of **20f** were obtained through slow crystallization from pentane at −35 °C. The ORTEP diagram of **20f** (Figure 4) indicates an Ir(III) octahedral complex with the CO bound in an apical site trans to the hydride and the aniline ligand trans to C_{ipso}. Since the crystal structure of **14f** showed an empty coordination site in the position trans to the hydride, CO coordination to this site is consistent with rapid addition of CO to generate **20f** as the kinetic product. Interestingly, there is a change in the orientation of the aniline ligand upon binding of CO. As mentioned earlier, in **14f** the dihedral angle H−Ir(1)−N(1)−H was 177°, with the hydride and *N*-H trans to each other. The dihedral angle H(1)−Ir(1)−N(11)−H(11) in **20f** after CO coordination is now 42°, indicating that the aniline ligand has rotated ca. 125° and the hydride and *N*-H are now nearly cis to each other.

Reaction of (POCOP)Ir(H)(NHAr-*p*CF_3) (**14e**) with CO was also investigated. Complex **14e** was generated in situ at 25 °C by treatment of tolyl hydrides **17** with $CF_3C_6H_4NH_2$ (ca. 1.5 equiv) at 25 °C. Cooling the toluene solution to −78 °C and purging with CO resulted in formation of four complexes. The major product was the expected CO addition product (POCOP)Ir(H)(CO)(NHC_6H_5-*p*-CF_3) (**20e**). The ^{1}H and ^{31}P NMR data support a structure analogous to **20f**. Two minor complexes corresponded to *p*- and *m*-tolyl hydride carbonyl complexes

(39) The stability of the aryl hydride complex can be dramatically altered by incorporation of fluorine substituents in the aromatic ring. In preliminary experiments we have shown that the reaction of (POCOP)Ir (**10**) with 2,3,5,6-tetrafluoroaniline yields *solely* the C−H activation product (POCOP)Ir(H)($C_6F_4NH_2$). Strengthening of the Re−aryl bond through fluorination of the aryl ring has been well-documented in earlier studies by Perutz et al. (*Chem. Commun.* **2003**, 490).

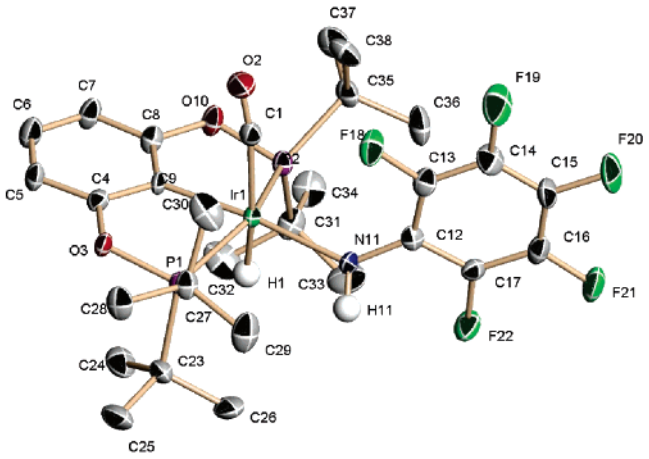

Figure 4. ORTEP diagram of (POCOP)Ir(H)(CO)(NHC_6F_5) (**20f**). Only the hydrogens on iridium and nitrogen are shown for clarity. Key bond distances (Å) and bond angles (deg): Ir(1)−N(11) = 2.168, N(11)−C(12) = 1.361, Ir(1)−C(9) = 2.046, Ir(1)−P(1) = 2.337, Ir(1)−P(2) = 2.329; H(1)−Ir(1)−N(11)−H(11) = 42.22, C(9)−Ir(1)−N(11) = 173.3, P(1)−Ir(1)−N(11) = 98.82, P(2)−Ir(1)−N(11) = 100.97, Ir(1)−N(11)−C(12)−C(13) = 139.79.

(POCOP)Ir(tolyl)(H)(CO). These structures were fully characterized by 2D ^{1}H NMR spectroscopy and independently generated by treatment of **17** with CO. Distinct ^{1}H NMR signals for these complexes are the downfield shifts (8.05−8.16 ppm) of the aryl protons ortho to Ir and the two Ir hydride triplets at −8.69 and −8.70 ppm. The fourth complex, also verified by independent synthesis, is (POCOP)Ir(H)(Cl)(CO), from CO trapping of unreacted starting material. By increasing the concentration of aniline used, formation of the tolyl complexes was inhibited. We were unable to crystallize **20e**, and column chromatography resulted in its decomposition.

Complex **20e** undergoes reductive elimination at a much slower rate than the five-coordinate analogue **14e**. Heating an in situ generated toluene-d_8 solution of (POCOP)Ir(H)(CO)(NHAr-*p*CF_3) (**20e**) at 63 °C results in the formation of (POCOP)Ir(CO) and free 4-(trifluoromethyl)aniline. In contrast, reductive elimination of five-coordinate **14e** occurs at 9 °C. A detailed kinetic analysis of the reductive elimination was not carried out, due to the difficulties in preparing **20e** cleanly and complications due to the presence of excess product aniline. However, qualitatively the rate of reductive elimination is retarded when carried out under 1−3 atm of carbon monoxide. This is consistent with loss of CO to form five-coordinate **14e** prior to reductive elimination, as might be expected on the basis of previous work concerning reductive elimination of six-coordinate Pt(IV) complexes.[40]

(II) Reaction of the (POCOP)Ir Pincer Complex with Benzamides $C_6H_5(CO)NH_2$ (21a) and $C_6F_5(CO)NH_2$ (21b). Reaction of (POCOP)Ir (**10**; generated by reaction of (POCOP)-Ir(H)(Cl) (**9**) with NaO*t*Bu) with $NH_2(CO)C_6H_5$ (**21a**) and NH_2-$(CO)C_6F_5$ (**21b**) yields the Ir(III) oxidative addition adducts **22a**,**b** (eq 12). These adducts are substantially more stable than the anilino hydrides and can be readily isolated as stable solids at room temperature.

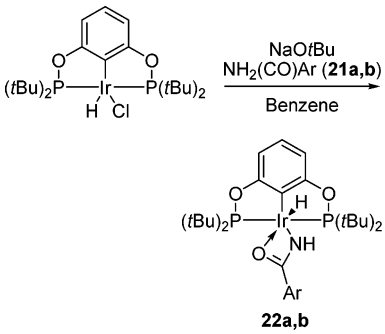

An X-ray diffraction study was carried out on a crystal of **22b** obtained from pentane at −35 °C. The ORTEP diagram is shown in Figure 6, along with key bond distances and angles. As for the anilino complexes, the amide nitrogen lies in the square plane trans to C_{ipso} of the aryl ring of the POCOP ligand. The N−C−O amide plane is perpendicular to the iridium square plane with the carbonyl oxygen anti to the axial Ir−H. The Ir−O bond distance of 2.55 Å suggests weak coordination of the amide oxygen to the open axial site trans to hydride. It is of interest to compare the iridium−oxygen bond distance in **22b** with Ir−O distances in the other iridium amide complexes **23**,[41] **24**,[42] and **25**,[43] shown in Figure 5. In the 18-electron Ir(III) complexes **23** and **24** the Ir−O distances of 3.401 and 3.412 Å clearly show no Ir−O interaction. The Ir(III) complex **25** is formally a 16-electron complex in the absence of a Ir−O interaction. The Ir−O distance of 2.290 Å is considerably shorter than the Ir−O distances in **23** and **24** and clearly suggests a significant bonding interaction. The fact that the amide in **25** is an alkyl amide with a much more basic oxygen then that in the benzamide of **22b** with a strongly electron-withdrawing C_6F_5 group may in part account for the shorter Ir−O distance in **25**.

The ^{1}H chemical shifts of the hydride ligands in **22a** and **22b** also support an axial Ir−O interaction. (POCOP)Ir hydride complexes with an empty coordination site trans to hydride exhibit hydride shifts in the −41 ppm range. In six-coordinate complexes the hydride shifts to much lower values. For example, in the carbonyl adduct **20f**, the ^{1}H shift is −8.56. The intermediate shifts of the hydrides in **22a** and **22b** of −30.25 and −35.72 ppm support a significant Ir−O interaction. The higher field shift of −35.7 ppm in **22b** suggests a decreased Ir−O interaction compared to that in **22a**, consistent with a decreased oxygen basicity due to the strongly electron-withdrawing C_6F_5 group.

(a) Rates of Reductive Elimination of $H_2N(CO)C_6H_5$ from (POCOP)Ir(H)(NH(CO)C_6H_5) Complexes. Since benzamides form significantly more stable Ir(III) species than their analogous anilino complexes, the rates of reductive elimination were measured at 100 °C. Ethylene proved to be a poor choice for a

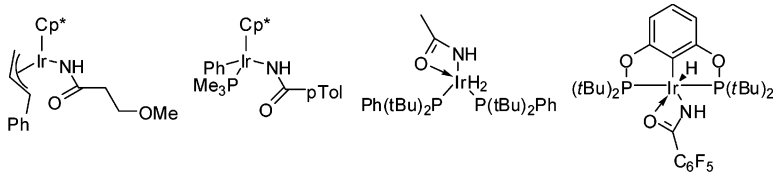

Figure 5. Comparison of Ir−O bond distances with those in the literature.

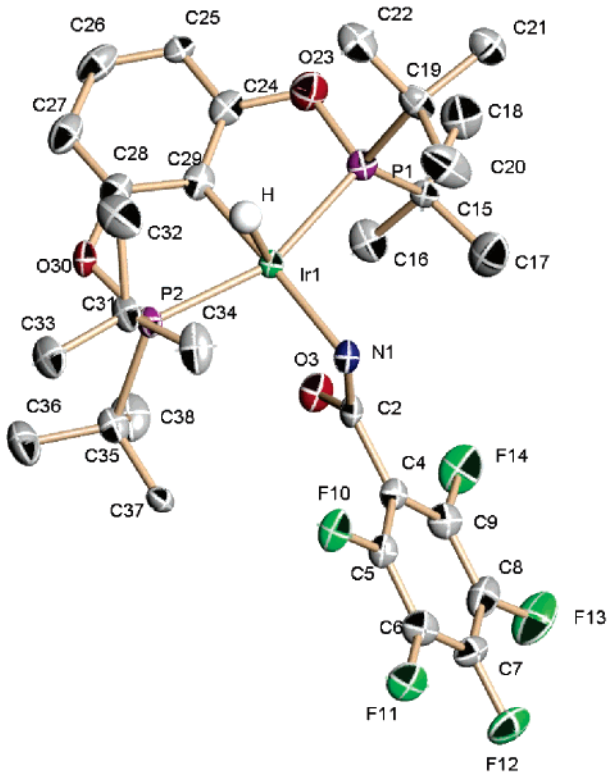

Figure 6. Crystal structure of (POCOP)Ir(H)(NH(CO)C_6F_5) (**22b**). Only the hydrogens on iridium are shown for clarity. Key bond distances (Å) and bond angles (deg): Ir(1)−N(1) = 2.171, N(1)−C(2) = 1.279, Ir(1)−C(29) = 2.034, Ir(1)−P(1) = 2.412, Ir(1)−P(2) = 2.359; H(1)−Ir(1)−N(1)−H(2) = −18.67, C(29)−Ir(1)−N(1) = 176.66, P(1)−Ir(1)−N(1) = 104.30, P(2)−Ir(1)−N(1) = 96.77, Ir(1)−N(1)−C(2)−C(4) = −175.64.

trapping ligand, since ethylene concentrations were difficult to control at elevated temperatures. Therefore, triphenylphosphine, which competes reversibly with benzamide for coordination to iridium, was used. The equilibrium between (POCOP)Ir(H)(NH(CO)Ph) (**22a**) + PPh_3 and (POCOP)Ir(PPh_3) + $H_2N(CO)C_6H_5$, as shown in eq 13, was measured at three different

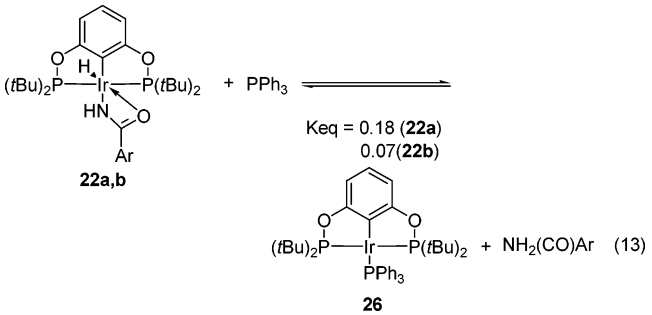

concentrations of PPh_3 (0.29, 0.59, and 1.18 M) at 100 °C. From these data a K_{eq} value of 0.18, favoring **22a**, was calculated. For the more electron-withdrawing pentafluorobenzamide complex **22b**, the equilibrium constant decreases to 0.07, consistent with the substituent effects observed in the aniline equilibrium studies. At room temperature benzamide **21a** (0.0094 M) and triphenylphosphine (0.0094 M) in a 1:1 ratio were added to **10** (0.0046 M), generated in the usual manner. ^{31}P NMR analysis showed the formation of **22a** and **26** in a ratio of 2:1. Since interconversion of these species is slow at 25 °C, this ratio represents kinetic trapping and differs from the thermodynamic ratio of ca. 6:1.

When **22a** was generated and the reversible reaction (eq 13) was analyzed in the presence of 10 equiv of **21a** and 10 equiv of PPh_3, the half-life for reductive elimination of benzamide was found to be ca. 1.7 h, corresponding to a $\Delta G^{\ddagger}$ value of ca. 29 kcal/mol. This increased barrier to reductive elimination of benzamide relative to that for anilines is due to stronger binding of the benzamido fragment to (POCOP)Ir. The Ir−O interaction as well as a decrease in the repulsive d_π−p interaction as a result of the electron-withdrawing ability of the acyl moiety can account for the increased binding energy.

Summary

Reaction of a series of anilines **11a**−**g** with (POCOP)Ir(C_6H_5)(H) (**12**) leads to equilibrium mixtures of **12**, the Ir(I) σ-complexes (POCOP)Ir(NH_2Ar) (**13**), and the Ir(III) oxidative addition adducts (POCOP)Ir(H)(NHAr) (**14**). Previous studies have shown that **12** undergoes rapid reductive elimination of benzene to form the 14-electron species (POCOP)Ir (**10**); therefore, complexes **13** and **14** arise from reaction of anilines with **10**. Equilibrium constants connecting these three species have been measured, and several features are apparent. As expected, as the basicity of the aniline increases, the equilibrium ratio (**13** + benzene):(**12** + aniline) increases. Surprisingly, however, as the basicity of the aniline decreases, the ratio of the Ir(III) species **14**, to Ir(I) species **13** increases, as does the ratio (**14** + benzene):(**12** + aniline). The increased stability of the oxidative addition adducts bearing electron-withdrawing aryl groups (-*p*-$CF_3C_6H_4$, **14e**; $-C_6F_5$, **14f**; 3,5-$(CF_3)_2C_6F_3$-, **14g**) was attributed to decreased repulsion between the filled d_π and N p orbitals.

Low-temperature NMR experiments employing *p*-chloroaniline show that reaction with **12** forms the Ir(I) σ-complex (POCOP)Ir($NH_2C_6H_4Cl$) (**13d**) as the kinetic product, which equilibrates with the oxidative addition adduct **14d** at temperatures above −50 °C. Complexes **14e**−**g** undergo reductive elimination at 9 °C in the presence of ethylene to yield quantitatively (POCOP)Ir(C_2H_4) (**18**) and the respective aniline. Rate measurements demonstrate that these reactions are cleanly first order and are independent of ethylene concentration. Mechanistic analysis suggests that the rate-determining step is formation of the σ-complex followed by loss of the aniline to form **10**, which is rapidly trapped by ethylene. The reductive elimination barriers of **14e**−**g** fall in the range of 21−22 kcal/mol and increase with the electron-withdrawing ability of the aryl groups.

Complex **14f** is square-pyramidal, with the hydride occupying the apical site. Trapping **14f** with CO forms the 18-electron complex (POCOP)Ir(H)(CO)(NHC_6F_5) (**20f**). X-ray analysis of a single crystal of **20f** indicates that CO has added at the vacant site trans to hydride. The six-coordinate CO adducts are much more stable with respect to reductive elimination. Complex **20e** undergoes reductive elimination at 63 °C at rates similar to **14e** reductive elimination at 9 °C. Qualitative rate measurements suggest CO must dissociate prior to reductive elimination.

Reaction of **12** with benzamides yields quantatively the Ir(III) oxidative addition adducts (POCOP)Ir(H)(NHC(O)Ar) (**22**). X-ray analysis of **22b** (Ar = C_6F_5) shows significant

(40) Crumpton-Bregel, D. M.; Goldberg, K. I. *J. Am. Chem. Soc.* **2003**, *125*, 9442.
(41) Chin, C. S.; Chong, D.; Lee, S.; Park, Y. J. *Organometallics* **2000**, *19*, 4043.
(42) Cooper, A. C.; Huffman, J. C.; Caulton, K. G. *Inorg. Chim. Acta* **1998**, *270*, 261.
(43) Tellers, D. M.; Ritter, J. C. M.; Bergman, R. G. *Inorg. Chem.* **1999**, *38*, 4810.

interaction of the carbonyl oxygen with Ir in the site trans to hydride. The barrier to reductive elimination of **22a**, 29 kcal/mol, is substantially higher than for complexes **14e**−**g**. The increased binding energy of the -NH(CO)Ar group to Ir is ascribed to Ir−O interaction as well as a decrease in the repulsive d_π−p interaction as a result of the strong electron-withdrawing ability of the acyl moiety.

Experimental Section

General Considerations. All manipulations were carried out using standard Schlenk, high-vacuum, and glovebox techniques. Argon and nitrogen were purified by passage through columns of BASF R3-11 (Chemalog) and 4 Å molecular sieves. THF was distilled from sodium benzophenone ketyl under nitrogen. Pentane and toluene were passed through columns of activated alumina and deoxygenated by purging with N_2. Benzene was dried with 4 Å molecular sieves and degassed by either freeze−pump−thaw methods or by purging with argon. Toluene was further treated by purging with argon to remove nitrogen. Toluene-d_8 and benzene-d_6 were dried over 4 Å molecular sieves and stored under argon in the glovebox. Hydrogen and carbon monoxide were used as received from National Specialty Gases of Durham, NC. NMR spectra were recorded on Bruker DRX 400 MHz and AMX 300 and 500 MHz instruments and are referenced to residual protio solvent peaks. ^{31}P chemical shifts are referenced to an external H_3PO_4 standard. Since there is a strong ^{31}P−^{31}P coupling in the pincer complexes, many of the ^{1}H and ^{13}C signals exhibit virtual coupling and appear as triplets. These are specified as vt with the *apparent* coupling simply noted as *J*. IR spectra were recorded on an ASI ReactIR 1000 spectrometer. Elemental analyses were carried out by Atlantic Microlab, Inc., of Norcross, GA. All reagents were purchased from Sigma-Aldrich and used without further purification. The POCOP bis(phosphinite) ligand and (POCOP)Ir(H)(Cl) (**9**) were prepared by literature procedures.[30] $[IrCODCl]_2$ can be purchased from Strem or synthesized using literature procedures.[44]

(POCOP)Ir(H)(Ph) (12). Complex **12** was generated in situ by treatment of (POCOP)Ir(H)(Cl) (**9**) with 1.1 equiv of NaOtBu in benzene at 75 °C for 30 min.[29]

General Procedure for the in Situ Generation of Complexes 13 and 14. (POCOP)Ir(H)(Cl) (**2**) was placed in a medium-walled screw-cap NMR tube with 1.1 equiv of NaO*t*Bu in 0.5 mL of benzene or toluene and heated to 75 °C for 45 min to generate the aryl hydride complex. The aniline was added to this mixture and allowed to react for 45 min at room temperature.

(POCOP)Ir(NH$_2$(*p*-OCH$_3$C$_6$H$_4$)) (13a). The general procedure was employed using **9** (0.033 mmol, 21 mg), NaO*t*Bu (0.037 mmol, 3.5 mg), and **11a** (0.099 mmol, 13.5 mg).

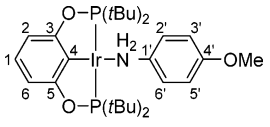

13a

^{1}H NMR (300 MHz, C_6D_6): δ 6.99 (d, $^3J_{H-H}$ = 8.7 Hz, 2H, 2′- and 6′-H), 6.95 (t, $^3J_{H-H}$ = 7.8 Hz, 1H, 1-H), 6.83 (d, $^3J_{H-H}$ = 7.8 Hz, 2H, 2- and 6-H), 6.59 (d, $^3J_{H-H}$ = 8.7 Hz, 2H, 3′- and 5′-H), 5.15 (s, 2H, $-NH_2$), 3.29 (s, 3H, OCH_3), 1.28 (vt, J = 6.5 Hz, 36H, 2 × P(*t*Bu)$_2$). ^{31}P{^{1}H} NMR (121.5 MHz, C_6D_6): δ 173.6. ^{13}C{^{1}H} NMR (75.5 MHz, C_6D_6): δ 167.9 (C_q, vt, J = 8.6 Hz, C3 and C5), 158.2 (C_q, s, C4′), 138.5 (C_q, s, C1′), 124.6 (CH, s, C3′ and C5′), 121.3 (CH, s, C1), 114.1 (CH, s, C2′ and C6′), 103.3 (CH, vt, J = 5.7 Hz, C2 and C6), 55.2 (CH_3, s, OCH_3), 41.1 (C_q, vt, J = 11.0 Hz, C(CH$_3$)$_3$), 28.6 (CH_3, vt, $^2J_{P-H}$ = 3.8 Hz, C(CH_3)$_3$). C4 not observed due to low intensity.

(POCOP)Ir(NH$_2$Ar-Me) (13b). The general procedure was employed using **9** (0.035 mmol, 22 mg), NaO*t*Bu (0.038 mmol, 3.9 mg), and **11b** (0.1 mmol, 11 mg).

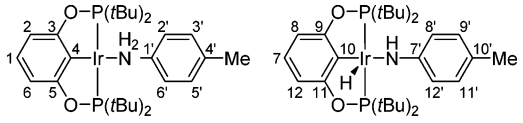

13b **14b**

^{1}H NMR (400 MHz, C_6D_6): **13b**, δ 6.77−6.96 (7H, aromatic protons), 5.17 (s, 2H, $-NH_2$), 2.04 (s, 3H, CH_3), 1.27 (vt, J = 6.4 Hz, 36H, 2 × P(*t*Bu)$_2$); the **14b** concentration is very low, resulting in the only distinguishing ^{1}H resonance as the hydride, δ −33.25 (t, J_{P-H} = 12.7 Hz, 1H, Ir−*H*). ^{31}P{^{1}H} NMR (121.5 MHz, C_6D_6): **13b**, δ 173.6; **14b**, δ 171.3. ^{13}C{^{1}H} NMR (100.6 MHz, C_6D_6): **13b**, δ 167.8 (C_q, vt, J = 8.7 Hz, C3 and C5), 144.7 (C_q, s, C1′), 135.3 (C_q, s, C4′), 129.4 (CH, s, C2′ and C6′), 127 (C_q, C4), 123.1 (CH, s, C3′ and C5′), 121.2 (CH, s, C1), 103.2 (CH, vt, J = 5.9 Hz, C2 and C6), 41.1 (C_q, vt, J = 11.0 Hz, C(CH$_3$)$_3$), 28.5 (CH_3, vt, J = 3.4 Hz, C(CH_3)$_3$), 20.6 (CH_3, s, CH_3).

(POCOP)Ir(NH$_2$C$_6$H$_5$) (13c)/(POCOP)Ir(H)(NHC$_6$H$_5$) (14c). The general procedure was employed using **9** (0.024 mmol, 15 mg), NaO*t*Bu (0.026 mmol, 2.5 mg), and **11c** (0.048 mmol, 4.4 μL). The equilibrating set of complexes **12**, **13c**, and **14c** as well as 10% of unreacted **9** were all present in the sample; thus, the ^{13}C NMR spectrum was not useful for structural assignments.

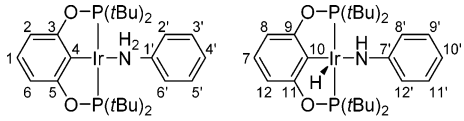

13c **14c**

^{1}H NMR (400 MHz, C_6D_6): **13c**, δ 6.69−6.96 (aromatic protons), 5.19 (s, 2H, NH_2), 1.26 (vt, J = 6.4 Hz, 36H, P(*t*Bu)$_2$); the concentration of **14c** is very low, resulting in the only distinguishing ^{1}H resonance as the hydride, δ −34.05 (t, J = 12.6 Hz). ^{31}P{^{1}H} NMR (162 MHz, C_6D_6): **13c**, δ 173.8; **14c**, δ 172.0.

(POCOP)Ir(NH$_2$(*p*-ClC$_6$H$_4$)) (13d)/(POCOP)Ir(H)(NH(*p*-Cl-C$_6$H$_4$)) (14d). The general procedure was employed using **9** (0.024 mmol, 15 mg), NaO*t*Bu (0.026 mmol, 2.5 mg), and **11d** (0.048 mmol, 6.1 μL). The equilibrating set **12**, **13d,** and **14d**, as well as 3% of unreacted **9**, were present in the NMR sample.

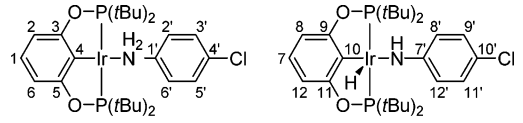

13d **14d**

^{1}H NMR (400 MHz, C_6D_6): δ 6.61−6.97 (m, 14H, aromatic protons for **13d** and **14d**), 5.60 (s, 1H, N*H*), 5.06 (s, 2H, NH_2), 1.08, 1.24 (m, 72H, P(*t*Bu)$_2$), −35.94 (t, J_{P-H} = 13.2 Hz, 1H, Ir−*H*). ^{31}P{^{1}H} NMR (162 MHz, C_6D_6): **13d**, δ 173.9; **14d**, δ 172.6.

(POCOP)Ir(H)(NH(*p*-CF$_3$C$_6$H$_4$)) (14e). The general procedure was employed using **9** (0.032 mmol, 20 mg), NaO*t*Bu (0.032 mmol, 3.1 mg), and **11e** (0.08 mmol, 10 μL).

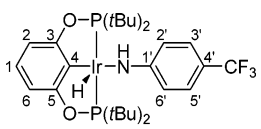

14e

^{1}H NMR (500 MHz, C_6D_6): δ 7.43 (d, $^3J_{H-H}$ = 8.5 Hz, 2H, 3′-

(44) Baghurst, D. R.; Mingos, D. M. P.; Watson, M. J. *J. Organomet. Chem.* **1989**, *368*, C43.

and 5′-H), 6.82 (t, $^3J_{H-H}$ = 7.8 Hz, 1H, 1-H), 6.73 (d, $^3J_{H-H}$ = 8.0 Hz, 2H, 2- and 6-H), 6.46 (d, $^3J_{H-H}$ = 8.5 Hz, 2H, 2′- and 6′-H), 4.37 (s, 1H, N*H*), 1.108 (vt, *J* = 7.5 Hz, 18H, P(*t*Bu)$_2$), 1.046 (vt, *J* = 7.0 Hz, 18H, P(*t*Bu)$_2$), −40.265 (t, J_{P-H} = 13.3 Hz, 1H, Ir−*H*). ^{31}P{^{1}H} NMR (162 MHz, C_6D_6): δ 173.3. ^{19}F NMR (376.5 MHz, C_6D_6): δ −59.1. ^{13}C{^{1}H} NMR (125.8 MHz, C_6D_6): δ 168.0 (C_q, vt, J_C = 5.5 Hz, C3 and C5), 164.0 (C_q, s, C1′), 127.0 (C_q, q, $^1J_{F-C}$ = 238.9 Hz, CF_3), 126.4 (CH, q, $^3J_{F-C}$ = 3.6 Hz, C3′ and C5′), 126.3 (CH, s, C1), 123.7 (C_q, br, C4), 117.1 (CH, s, C2′ and C6′), 112.7 (C_q, q, $^2J_{F-C}$ = 32.2 Hz, C4′), 104.8 (CH, t, J_{P-H} = 5.2, C2 and C6), 42.7 (Cq, vt, *J* = 10.8 Hz, *C*(CH$_3$)$_3$), 38.9 (Cq, vt, *J* = 12.8 Hz, *C*(CH$_3$)$_3$), 28.0 (CH$_3$, vt, *J* = 3.2 Hz, C(*C*H$_3$)$_3$), 27.6 (CH$_3$, vt, J_{P-H} = 3.2 Hz, C(*C*H$_3$)$_3$).

(POCOP)Ir(H)(NHC$_6$F$_5$) (14f). Simultaneously, **9** (0.034 mmol, 21 mg), NaO*t*Bu (0.037 mmol, 3.6 mg), **11f** (0.068 mmol, 12.4 mg), and benzene-d_6 (0.5 mL) were added to a medium-walled screw-cap NMR tube and heated to 75 °C for 1 h.

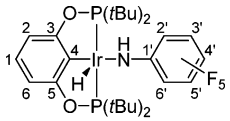

14f

^{1}H NMR (500 MHz, C_6D_6): δ 6.82−6.72 (m, 3H, 1-, 2-, 6-H), 3.01 (s, 1H, N*H*), 1.09−1.03 (m, 36H, P(*t*Bu)$_2$), −42.15 (t, J_{P-H} = 13.5 Hz, 1H, Ir−*H*). ^{31}P{^{1}H} NMR (162 MHz, C_6D_6): δ 172.8. ^{19}F NMR (376.5 MHz, C_6D_6): δ −167.3 (m), −168.9 (m), −187.3 (m). ^{13}C{^{1}H} NMR (125.8 MHz, C_6D_6): δ 168.5 (C_q, vt, *J* = 5.5 Hz, C3 and C5), 140.4−135.8 (m, C_q, Ar−F$_5$: C2′, C6′, C3′, C5′, and C4′), 126.7 (CH, s, C1), 122.6 (C_q, t, C4), 104.9 (CH, t, J_{P-H} = 5.3 Hz, C2 and C6), 42.6 (Cq, vt, *J* = 11.1 Hz, *C*(CH$_3$)$_3$), 39.1 (Cq, vt, *J* = 12.6 Hz, *C*(CH$_3$)$_3$), 27.7 (CH$_3$, vt, *J* = 3.2 Hz, C(*C*H$_3$)$_3$), 27.2 (CH$_3$, vt, *J* = 3.0 Hz, C(*C*H$_3$)$_3$), C1′ not observed due to low intensity.

(POCOP)Ir(H)(NH(3,5-(CF$_3$)$_2$C$_6$H$_3$)) (14g). The general procedure was employed using **9** (0.035 mmol, 22 mg), NaO*t*Bu (0.039 mmol, 3.7 mg), and **11g** (0.07 mmol, 10.9 μL).

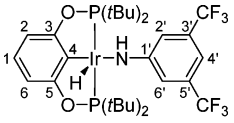

14g

^{1}H NMR (500 MHz, C_6D_6): δ 6.98 (s, 1H, 4′-H), 6.87 (s, 2H, 2′- and 6′-H), 6.81 (t, $^3J_{H-H}$ = 7.9 Hz, 1H, 1-H), 6.73 (d, $^3J_{H-H}$ = 7.9 Hz, 2H, 2- and 6-H), 3.74 (s, 1H, N*H*), 1.06 (vt, *J* = 7.4 Hz, 18H, P(*t*Bu)$_2$), 0.99 (vt, *J* = 6.8 Hz, 18H, P(*t*Bu)$_2$), −41.77 (t, J_{P-H} = 13.5 Hz, 1H, Ir−*H*). ^{31}P{^{1}H} NMR (162 MHz, C_6D_6): δ 174.0 (d). ^{19}F NMR (376.5 MHz, C_6D_6): δ −63.2. ^{13}C{^{1}H} NMR (125.8 MHz, C_6D_6): δ 168.5 (C_q, vt, *J* = 5.6 Hz, C3 and C5), 161.4 (C_q, s, C1′), 132.0 (C_q, q, $^2J_{F-C}$ = 31.4 Hz, C3′ and C5′), 127.0 (CH, s, C1), 125.5 (C_q, q, $^1J_{F-C}$ = 273.3 Hz, *C*F$_3$), 124.5 (C_q, m, C4), 115.7 (CH, m, C2′ and C6′), 105.0 (CH, t, vt, *J* = 5.2 Hz, C2 and C6), 102.4 (CH, septet, $^3J_{F-C}$ = 4.0 Hz), 42.8 (Cq, vt, *J* = 10.9 Hz, *C*(CH$_3$)$_3$), 38.7 (Cq, vt, *J* = 12.8 Hz, *C*(CH$_3$)$_3$), 28.0 (CH$_3$, vt, *J* = 3.2 Hz, C(*C*H$_3$)$_3$), 27.3 (CH$_3$, vt, *J* = 3.1 Hz, C(*C*H$_3$)$_3$).

General Procedure for Determining the Equilibrium Constants *K*$_1$, *K*$_2$, and *K*$_3$ (Scheme 1). Samples were prepared as described below in benzene. Molarities of species were determined by carefully measuring the final volume of the solution. Both ^{1}H and ^{31}P spectra were used to determine ratios of species. ^{31}P spectra were taken with a delay time of 15 s to ensure the integrals were accurate on the basis of the 5 × T1 value of **14f**.

Reaction of (POCOP)Ir(H)(C$_6$H$_5$) (12) and *p*-CH$_3$OC$_6$H$_4$NH$_2$ (11a). To a vial in the glovebox under argon, **9** (0.088 mmol, 55.35 mg), NaO*t*Bu (0.8 equiv, 0.07 mmol, 6.0 mg), **11a** (0.041 mmol, 5.1 mg, 0.010 M), and benzene (4 mL) were added. The reaction mixture was stirred for 1.5 h. An aliquot was removed and analyzed by ^{31}P NMR. The equilibrium constants were calculated on the basis of the concentrations of all the species in solution, (K_1 = 1014, K_2 = n/a). A second aliquot was removed after another 1 h to ensure the reaction was at equilibrium. The reaction was repeated with an increase in the concentration of **11a** to 0.05 M (K_1 = 1189, K_2 = n/a). No **14a** could be detected.

Reaction of (POCOP)Ir(H)(C$_6$H$_5$) (12) and *p*-CH$_3$C$_6$H$_4$NH$_2$ (11b). The general procedure for **11a** was followed using **9** (0.069 mmol, 43.45 mg), NaO*t*Bu (0.9 equiv, 0.062 mmol, 6.0 mg), **11b** (0.20 mmol, 21.43 mg, 0.050 M), and benzene (4 mL) (K_1 = 462, K_2 = 0.04). The reaction was repeated with an increase in the concentration of **11b** to 0.10 M (K_1 = 448, K_2 = 0.04).

Reaction of (POCOP)Ir(H)(C$_6$H$_5$) (12) and C$_6$H$_5$NH$_2$ (11c). The general procedure for **11a** was followed using **9** (0.075 mmol, 46.9 mg), NaO*t*Bu (0.9 equiv, 0.067 mmol, 6.47 mg), **11c** (0.2 mmol, 0.18 μL, 0.050 M), and benzene (4.0 mL) (K_1 = 188, K_2 = 0.07). The reaction was repeated with an increase in the concentration of **11c** to 0.10 M (K_1 = 189, K_2 = 0.08).

Reaction of (POCOP)Ir(H)(C$_6$H$_5$) (12) and *p*-ClC$_6$H$_4$NH$_2$ (11d). The general procedure for **11a** was followed using **9** (0.074 mmol, 46.15 mg), NaO*t*Bu (0.9 equiv, 0.066 mmol, 6.4 mg), **11d** (0.392 mmol, 50 mg, 0.10 M), and benzene (4 mL) (K_1 = 50, K_2 = 1). The reaction was repeated with an increase in the concentration of **11d** to 0.15 mol/L (K_1 = 60, K_2 = 1).

Reaction of (POCOP)Ir(H)(C$_6$H$_5$) (12) and *p*-CF$_3$C$_6$H$_4$NH$_2$ (11e). The general procedure for **11a** was followed using **9** (0.138 mmol, 86.6 mg), NaO*t*Bu (0.9 equiv, 0.124 mmol, 11.9 mg), **11e** (0.08 mmol, 12.9 mg, 0.010 M), and benzene (8 mL) (K_3 = 272). The reaction was repeated with an increase in the concentration of **11e** to 0.050 M (K_3 = 259). No **13e** could be detected.

Reaction of (POCOP)Ir(H)(C$_6$H$_5$) (12) and C$_6$F$_5$NH$_2$ (11f). The general procedure for **11a** was followed using **9** (0.038 mmol, 23.75 mg), NaO*t*Bu (0.9 equiv., 0.0343 mmol, 3.3 mg), **11f** (0.0721 mmol, 13.2 mg, 0.009 M), and benzene (8 mL) was added (K_3 = 2010). The reaction was repeated with an increase in the concentration of **11f** to 0.012 M (K_3 = 2300). No **13f** could be detected.

Reaction with (POCOP)Ir(H)(C$_6$H$_5$) (12) and 3,5-(CF$_3$)$_2$-C$_6$H$_3$NH$_2$ (11g). The general procedure for **11a** was followed using **9** (0.158 mmol, 99.05 mg), NaO*t*Bu (0.9 equiv, 0.142 mmol, 13.65 mg), **11g** (0.08 mmol, 18 mg, 0.010 M), and benzene (8 mL) (K_3 = 2700). The reaction was repeated with an increase in the concentration of **11g** to 0.050 M (K_3 = 2850). No **13g** could be detected.

Low-Temperature Oxidative Addition of *p*-Chloroaniline to 10. In a screw cap NMR tube, **10** was generated by reaction of **9** (0.023 mmol, 15 mg) with NaO*t*Bu (0.023 mmol, 2.3 mg) in 0.4 mL of toluene-d_8 at 100 °C for 1 h. The reaction mixture was cooled to −78 °C in a dry ice/acetone bath, and 0.1 mL of a 2.3 M solution of *p*-chloroaniline (0.23 mmol) was added via syringe. The reaction mixture was warmed in the NMR probe until the solution consisted solely of **13c**, after which the oxidative addition was monitored at −12 °C. A data plot is included in the Supporting Information.

Kinetic Analysis of the Reductive Elimination Reactions of 14e−g. In a screw-cap NMR tube, **10** was generated by reaction of **9** (0.023 mmol, 15 mg) with NaO*t*Bu (0.023 mmol, 2.3 mg) in 0.5 mL of toluene-d_8 at 100 °C for 1 h. Anilines **11e−g** were added to the solution of **10** and allowed to react for 45 min. The NMR tube was cooled to −78 °C in a dry ice/acetone bath, followed by addition of ethylene to the reaction mixture via syringe. The NMR tube was warmed to 9 °C in the probe, and the reductive elimination was monitored by ^{1}H NMR spectroscopy. A plot of kinetic data for **14f** is included in the Supporting Information.

Kinetic Analysis of the Dissociation of H$_2$NC$_6$H$_4$-*p*OMe (11a) from 13a. (POCOP)Ir(H)(Cl) (**9**; 10 mg, 0.016 mmol), NaO*t*Bu (1.7 mg, 0.018 mmol), and toluene-d_8 (0.4 mL) were heated for 1

h. at 100 °C in a J. Young NMR tube to generate the tolyl hydride complexes **17**. *p*-Methoxyaniline (**11a**; 3.5 mg, 0.024 mmol) and 1,3,5-trimethoxybenzene (0.1 mL, 0.11 M solution in toluene-d_8) was added to the NMR tube. After the NMR sample was freeze−pump−thawed, ethylene (10−20 equiv, 3.6−7.2 mL at 23 °C) was introduced via a gastight syringe at liquid-nitrogen temperature. The reaction was then monitored via low-temperature NMR spectroscopy at −8 °C. A plot of kinetic data is included in the Supporting Information.

(POCOP)Ir(H)(NHC$_6$F$_5$)(CO) (20f). In a Schlenk flask, **9** (101 mg, 0.16 mmol), NaO*t*Bu (17 mg, 0.18 mmol), **11f** (33 mg, 0.18 mmol), and toluene (5 mL) were added and stirred at room temperature for 1 h. The reaction mixture was cooled to −78 °C, and then CO was purged through the solution until the color lightened. The toluene was removed under vacuum, and the product was extracted with pentane. The pentane was reduced under vacuum until the product began to precipitate. The pentane was then cooled to −78 °C, and the precipitate was filtered and washed with cold pentane (60 mg, 46% yield).

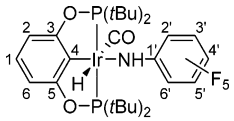

20f

^{1}H NMR (500 MHz, C_6D_6): δ 6.74 (t, $^3J_{H-H}$ = 8.0 Hz,1H, 1-H), 6.59 (d, $^3J_{H-H}$ = 8.0 Hz, 2H, 2- and 6-H), 2.33 (s, 1H, N*H*), 1.20 (vt, J_{P-H} = 7.7 Hz, 18H, P(*t*Bu)$_2$), 1.11 (vt, J_{P-H} = 7.3 Hz, 18H, P(*t*Bu)$_2$), −8.56 (t, J_{P-H} = 17.9 Hz, 1H, Ir−*H*). ^{31}P{^{1}H} NMR (162 MHz, C_6D_6): δ 57.6. ^{19}F NMR (376.5 MHz, C_6D_6): δ −163.3 (bs), −169.0 (t), −186.7 (septet). ^{13}C{^{1}H} NMR (125.8 MHz, C_6D_6): δ 179.4 (C_q, *C*═O), 163.8 (C_q, vt, J_{P-C} = 3.7 Hz, C3 and C5), 140.4−135.8 (m, C_q, Ar−F_5: C2′, C6′, C3′, C5′, and C4′), 126.8 (CH, s, C1), 106.0 (CH, t, vt, J_{P-H} = 4.8 Hz, C2 and C6), 43.0 (Cq, vt, J_{P-H} = 12.6 Hz, *C*(CH$_3$)$_3$), 40.6 (Cq, vt, J_{P-H} = 11.4 Hz, *C*(CH$_3$)$_3$), 28.1 (CH$_3$, vt, J_{P-H} = 2.9 Hz, C(*C*H$_3$)$_3$), 27.2 (CH$_3$, vt, J_{P-H} = 2.4 Hz, C(*C*H$_3$)$_3$). C4 and C1′ were not observed, due to low intensity. IR (C_6D_6): 2022 cm^{-1}. Anal. Calcd for $C_{29}H_{41}O_3P_2N_1F_5Ir$ (800.80): C, 43.50; H, 5.16; N, 1.75. Found: C, 43.70; H, 5.25; N: 1.71.

Reductive Elimination of *p*-(Trifluoromethyl)aniline from (POCOP)Ir(H)(CO)(NHC$_6$H$_4$-*p*CF$_3$) (20e). In a J. Young NMR tube, tolyl complexes **17** were generated by heating the reaction mixture of (POCOP)Ir(H)(Cl) (**9**; 15 mg, 0.024 mmol), NaO*t*Bu (2.3 mg, 0.024 mmol), and 0.5 mL of toluene-d_8 for 1 h at 100 °C. The reaction mixture was cooled to room temperature. The addition of *p*-(trifluoromethyl)aniline (**11e**; 6.0 μL, 0.048 mmol) formed complex **14e**. After the reaction mixture was freeze−pump−thawed, a gastight syringe was used to add sufficient CO at liquid-N_2 temperature to generate pressures of 1, 2, and 3 atm of CO in the headspace at 25 °C. The reaction was monitored at 63 °C by ^{1}H NMR spectroscopy.

Procedure for Monitoring the Reaction of Benzamide Complex 22a with PPh$_3$. A stock solution of (POCOP)Ir(H)(NH(CO)-Ar) was prepared in the glovebox under Ar by stirring (POCOP)-Ir(H)(Cl) (**9**; 112.7 mg, 0.18 mmol), NaO*t*Bu (20.7 mg, 0.22 mmol), benzamide **21a** (26.2 mg, 0.22 mmol), and toluene-d_8 (3.0 mL) until the solution turned pale orange: ca. 30 min. The excess benzamide and NaO*t*Bu were filtered out through a 0.02 μm syringe filter. The concentration of the stock solution (0.063 M) was measured via ^{1}H NMR using 2.0 μL of mesitylene as a standard. Aliquots (0.5 mL) of the stock solution were added to three J. Young NMR tubes containing known amounts of PPh$_3$ (0.147 mmol, 0.294 mmol, 0.588 mmol). The NMR tubes were heated to 100 °C for 3 days, after which the reaction was stopped by placing the NMR tubes in cold water. The K_{eq} value was calculated by measuring the ratios of **22a** and **26** by ^{31}P NMR. K_{eq} = 0.18.

Procedure for Monitoring the Reaction of Benzamide Complex 22b with PPh$_3$. A stock solution was prepared using **9** (92.5 mg, 0.148 mmol), NaO*t*Bu (71.0 mg, 0.74 mmol), **22b** (161.6 mg, 0.74 mmol), and toluene-d_8 (6.0 mL). Aliquots of the stock solution (0.6 mL, 0.021 M) were placed in three J. Young tubes with known amounts of PPh$_3$ (0.126, 0.252, 0.378 mmol). The reaction mixtures were heated to 100 °C overnight, after which the reactions were stopped by placing the NMR tubes in cold water. The K_{eq} value was calculated by measuring the ratios of **22b** and **26** by ^{31}P NMR. K_{eq} = 0.067.

(POCOP)Ir(PPh$_3$) (24). In a Schlenk flask **9** (104 mg, 0.166 mmol), NaO*t*Bu (17.6 mg, 0.183 mmol), PPh$_3$ (46 mg, 0.174 mmol), and toluene (10 mL) were combined and stirred overnight. Toluene was removed under vacuum until the product precipitated. The product was filtered, washed with cold toluene, and dried under vacuum to yield an orange solid (74 mg, 52% yield). ^{1}H NMR (500 MHz, C_6D_6): δ 8.06 (t, 6H, PPh$_3$), 6.9−7.1 (m, 12H, aromatic protons), 1.072 (vt, J_{P-H} = 6.8 Hz, 36H, P(*t*Bu)$_2$). ^{31}P{^{1}H} NMR (162 MHz, C_6D_6): δ 181.2 (d, J_{P-P} = 5.2 Hz), 15.8 (t, J_{P-P} = 5.5 Hz). ^{13}C{^{1}H} NMR (100.6 MHz, C_6D_6): δ 166.4 (C_q, vt, J_{P-C} = 6.5 Hz, C3 and C5), 141.5, 135.7, 133.7, 129, 127.0, 125.7 (CH, s, C1), 102.7 (CH, t, vt, C2 and C6), 41.0 (Cq, vt, J_{P-H} = 11.6 Hz, *C*(CH$_3$)$_3$), 28.7 (CH$_3$, s). Anal. Calcd for $C_{40}H_{54}O_2P_3Ir$ (851.99): C, 56.39; H, 6.39. Found: C, 56.19; H, 6.37. Crystallographic data are included in the Supporting Information.

Kinetic Analysis of the Reductive Elimination of Benzamide 22a. A stock solution (0.06 M) of (POCOP)Ir(H)(NH(CO)C$_6$H$_5$) (**23a**) was prepared under Ar by stirring (POCOP)Ir(H)(Cl) (**9**; 75.1 mg, 0.12 mmol), NaO*t*Bu (12.7 mg, 0.132 mmol), benzamide **22a** (16.0 mg, 0.132 mmol), and toluene-d_8 (2 mL) until the solution turned pale orange. The excess benzamide and NaO*t*Bu were filtered out through a 0.02 μm syringe filter. In a screw-cap NMR tube, 10 equiv of **22a** (15 mg, 0.124 mmol), 10 equiv of PPh$_3$ (32.5 mg, 0.124 mmol), the stock solution of **23a** (0.21 mL, 0.06 M), and toluene-d_8 (0.4 mL) were added. The reaction mixture was heated to 100 °C in the NMR probe, and over time the disappearance of **23a** signals was monitored via ^{1}H NMR. A plot of kinetic data is included in the Supporting Information.

(POCOP)Ir(H)(NH(CO)(Ph) (22a). (POCOP)Ir(H)(Cl) (**9**; 100 mg, 0.16 mmol), NaO*t*Bu (18.4 mg, 0.192 mmol), H$_2$N(CO)C$_6$H$_5$ (**21a**; 23.2 mg, 0.192 mmol), and 5.0 mL of benzene were added to a Schlenk flask, and the mixture was stirred for 1.5 h until the color changed to a light orange. The solution was filtered though a 0.2 μm syringe filter, and the benzene was sublimed at 0 °C to yield a yellow-orange solid (71.6 mg, 63% yield).

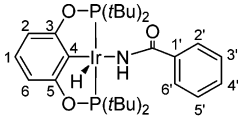

22a

^{1}H NMR (500 MHz, C_6D_6): δ 7.64−7.62 (m, 2H, 2′- and 6′-H), 7.12−7.07 (m, 3H, 3′-, 4′, and 5′-H), 6.87−6.79 (m, 3H, 1-, 2-, and 3-H), 5.90 (bs, 1H, N*H*), 1.40 (vt, J_{P-H} = 6.9 Hz, 18H, P(*t*Bu)$_2$), 1.28 (vt, J_{P-H} = 7.0 Hz, 18H, P(*t*Bu)$_2$), −30.25 (t, J_{P-H} = 13.2 Hz, 1H, Ir−*H*). ^{31}P{^{1}H} NMR (162 MHz, C_6D_6): δ 164.2. ^{13}C-{^{1}H} NMR (125.8 MHz, C_6D_6): δ 176.4 (C_q, t, J_{P-C} = 1.3 Hz, *C*O), 166.6 (C_q, vt, J_{P-C} = 6.0 Hz, C3 and C5), 138.4 (C_q, s, C1′), 130.1 (CH, s, C4′), 128.3 (CH, s, C3′ and C5′), 126.3 (CH, s, C2′ and C6′), 124.1 (CH, s, C1), 118.5 (C4), 104.5 (CH, t, J_{P-C} = 5.4 Hz, C2 and C6), 42.5 (Cq, vt, J_{P-H} = 12.0 Hz, *C*(CH$_3$)$_3$), 39.9 (Cq, vt, J_{P-H} = 11.8 Hz, *C*(CH$_3$)$_3$), 28.8 (CH$_3$, vt, J_{P-H} = 3.3 Hz, C(*C*H$_3$)$_3$), 27.6 (CH$_3$, bvt, J_{P-H} = 2.2 Hz, C(*C*H$_3$)$_3$). Anal. Calcd for $C_{29}H_{46}O_3P_2NIr$ (710.85): C, 49.00; H, 6.52; N, 1.97. Found: C, 49.22; H, 6.59; N, 2.00.

(POCOP)Ir(H)(NH(CO)(C$_6$F$_5$) (22b). (POCOP)Ir(H)(Cl) (**9**; 100 mg, 0.16 mmol), NaO*t*Bu (18.4 mg, 0.192 mmol), H$_2$N(CO)-

C_6F_5 (**21b**; 40.5 mg, 0.192 mmol), and 5.0 mL of benzene were added to a Schlenk flask, and the mixture was stirred for 1.5 h until the color changed to a light orange. The solution was filtered though a 0.2 μm syringe filter, and the benzene was sublimed at 0 °C to yield a yellow-orange solid (101.6 mg, 79% yield).

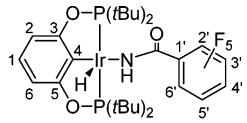

22b

^{1}H NMR (500 MHz, C_6D_6): δ 6.87−6.78 (m, 3H, 1-, 2-, 6-H), 5.49 (bs, 1H, N*H*), 1.44 (vt, J_{P-H} = 7.0 Hz, 18H, P(*t*Bu)$_2$), 1.22 (vt, J_{P-H} = 7.0 Hz, 18H, P(*t*Bu)$_2$), −35.72 (t, J_{P-H} = 13.0 Hz, 1H, Ir−*H*). ^{19}F NMR (376.5 MHz, C_6D_6): δ −141.76 (m), −155.25 (m), −166.61 (m). ^{13}C{^{1}H} NMR (125.8 MHz, C_6D_6): δ 167.2 (C_q, vt, J_{P-C} = 5.8 Hz, C3 and C5), 163.0 (C_q, s, *C*O), 144.5 (C_q, dm, $^1J_{F-C}$ = 241.8 Hz, C2′ and C6′), 141.1 (C_q, dm, $^1J_{F-C}$ = 254.3 Hz, C4′), 137.7 (C_q, dm, $^1J_{F-C}$ = 252.0 Hz, C3′ and C5′), 125.4 (CH, s, C1), 119.9 (C_q, m, C4), 116.2 (C_q, m, C1′), 104.7 (CH, t, vt, J_{P-H} = 5.3 Hz, C2 and C6), 42.8 (Cq, vt, J_{P-H} = 12.1 Hz, *C*(CH$_3$)$_3$), 39.8 (Cq, vt, J_{P-H} = 12.1 Hz, *C*(CH$_3$)$_3$), 28.3 (CH$_3$, vt, J_{P-H} = 3.3 Hz, C(*C*H$_3$)$_3$), 27.6 (CH$_3$, vt, J_{P-H} = 3.1 Hz, C(*C*H$_3$)$_3$). Anal. Calcd for $C_{29}H_{41}O_3P_2NF_5Ir$ (800.80): C, 43.50; H, 5.16; N, 1.75. Found: C, 43.70; H, 5.25; N, 1.71.

Acknowledgment. We gratefully acknowledge funding by the National Institutes of Health (Grant No. GM 28938).

Supporting Information Available: CIF files containing X-ray crystallographic data for complexes **14f**, **20f**, **22b**, and **26** and figures giving kinetic plots for the conversion of **13d** to **14d**, for the dissociation of **11a** from **13a**, for the reductive elimination of **11f** from **14f**, and for the reductive elimination of benzamide from **22a**. This material is available free of charge via the Internet at http://pubs.acs.org.

OM051070N